Polymer 49 (2008) 2636–2643

Contents lists available at ScienceDirect

Polymer

journal homepage: www.elsevier.com/locate/polymer

Photopolymerization kinetics of poly(acrylate)–clay composites using polymerizable surfactants

Kwame Owusu-Adom, C. Allan Guymon*

Department of Chemical & Biochemical Engineering, University of Iowa, 4133 Seamans Center, Iowa City, IA 52241, United States

ARTICLE INFO

Article history:
Received 20 November 2007
Received in revised form 27 March 2008
Accepted 29 March 2008
Available online 3 April 2008

Keywords:
Photopolymerization
Kinetics
Polymerizable surfactants

ABSTRACT

Photopolymerization kinetics of polymer–clay nanocomposite systems utilizing polymerizable quaternary ammonium surfactants as dispersants were systematically investigated to determine the effects of surfactant type and clay morphology on polymerization behavior. For these studies, either polymerizable surfactants were mixed into a clay–monomer system or the surfactants were ionically anchored to clay surfaces and added to the monomer for *in situ* photopolymerization. Higher photopolymerization rates are observed with increasing polymerizable surfactant concentration, while no significant change or decreases in polymerization rate occur with incorporation of non-polymerizable surfactants. The higher rates observed for polymerizable surfactant systems are due to lower apparent termination rate parameters stemming from immobilization of the surfactants. For clay that is modified with ionically bonded quaternary ammonium surfactants, polymerization rates decrease in both polymerizable and non-polymerizable organoclay systems with increasing concentration, but this decrease is much smaller when polymerizable organoclays are utilized. For the same organoclay concentration, higher polymerization rates and double bond conversions result with increasing polymerizable surfactant concentration via cation exchange. Significant increases in polymerization rate also occur with increasing degree of clay exfoliation.

1. Introduction

Polymer–clay nanocomposites continue to attract significant research interest due to the potential of enhanced modulus, heat distortion temperature, and optical and gas barrier properties with incorporation of low clay concentrations [1–4]. The improved material properties have been attributed to polymer–clay interactions based on inherent nanoscale dimensions of the clay platelets. One commonly examined clay, montmorillonite, is composed of negatively charged sheets of the 2:1 phyllosilicate family. Individual sheets are approximately 1 nm thick and vary in lateral dimension from 50 nm to several microns. The negatively charged platelets are counterbalanced by exchangeable cations in the gallery between adjacent sheets. These sheets are held together by ionic interactions with separation on the order of van der Waals' distance in the stacked sheets [1,3]. Cation exchange procedures are used to modify clay surfaces often with quaternary ammonium surfactants to enhance clay miscibility in organic systems [1]. Different clay dispersion states in such polymer systems are commonly observed: an intercalated morphology in which the clay retains its ordered structure with polymer embedded in the interlayers, and complete delamination of the clay platelets to form exfoliated nanocomposites, or combinations of the two. Enhanced physical, mechanical, thermal and optical properties have been attributed primarily to the exfoliated clay state [1–5].

Promise of significant property improvements upon clay addition has led to the development of many polymer–clay nanocomposite materials, some of which are formed via *in situ* polymerization [3,5–8]. While much attention has been devoted to the development of exfoliated nanocomposites, fundamental understanding of the role of clay morphology on the reaction kinetics in polymer–clay nanocomposites formed *in situ* has not been examined to any significant degree. Other research has shown interesting reaction dynamics in polymerization within ordered nanoscopic domains. For example, polymerization in the ordered domains of both lyotropic and thermotropic liquid crystalline (LC) systems results in different kinetic behaviors that are dependent on the LC morphology [9–11]. The periodic order in clay particles may also induce similar changes in polymerization behavior that could influence final nanocomposite properties. In addition, the large aspect ratio of clay particles could induce interesting polymerization dynamics from interactions with the constituents of the polymerizing system. Influence of such interactions has been observed in template polymerizations in which the presence of templating domains affords enhanced reaction rates [12]. For *in situ* polymerizations such as photopolymerization, understanding

* Corresponding author. Tel.: +1 319 335 5015; fax: +1 319 335 1415.
E-mail address: cguymon@engineering.uiowa.edu (C.A. Guymon).

0032-3861/$ – see front matter © 2008 Elsevier Ltd. All rights reserved.
doi:10.1016/j.polymer.2008.03.045

these interactions could be vital in designing appropriate photopolymer–clay nanocomposites. Photopolymerization may be ideal for forming nanocomposites based on the inherent speed of photopolymerization, spatial and temporal control of initiation and temperature-independent initiation.

The state of clay dispersion may change photopolymerization behavior through the amount of light scattered or absorbed by agglomerated clay particles. Surfactant and clay interactions could modify the polymerization environment through interactions with the bulk monomer. With reactive functionalities, the surfactants could be used to control overall material properties as they polymerize into the bulk polymer network [13,14]. This study investigates the photopolymerization kinetics of polymer–clay nanocomposites containing various quaternary ammonium surfactants. Influence of the ordered clay morphology, concentration and type of surfactant, as well as clay–surfactant interactions on photopolymerization behavior, is investigated. In particular, photopolymerization rates with the use of polymerizable surfactants in combination with the ordered clay morphology in clay-polymer systems are examined. Propagation and termination rate parameters are determined to explain observed photopolymerization kinetic behavior. Through this study, the effect of polymerizable dispersants and state of clay agglomeration on polymerization behavior in photopolymerizable clay nanocomposites is determined.

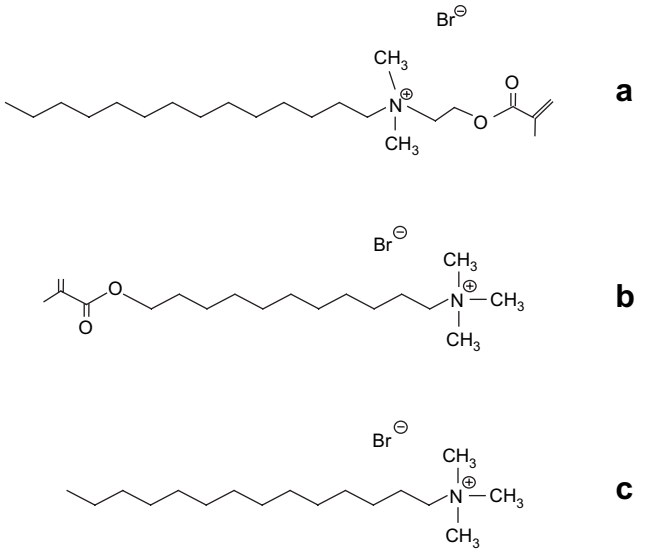

Fig. 1. Chemical structures of (a) tetradecylethylmethacrylate dimethylammonium bromide (C14MA), (b) undecylmethacrylate trimethylammonium bromide (PM1) and (c) tetradecyltrimethylammonium bromide (TTAB) surfactants.

2. Experimental

2.1. Materials

Sodium montmorillonite (Cloisite Na^+, clay) was purchased from Southern Clay Products. Tetradecyltrimethylammonium bromide (TTAB, Aldrich), 1,6-hexanediol diacrylate (HDDA) and tripropylene glycol diacrylate (TrPGDA, Aldrich) were used as-received. TTAB was used as a model non-polymerizable surfactant in studying the polymerization behavior of clay–monomer mixtures. Tetradecylethylmethacrylate dimethylammonium bromide (C14MA), and undecylmethacrylate trimethylammonium bromide (PM1), two types of methacrylated quaternary ammonium surfactants, were synthesized as described previously [15,16]. The free radical photoinitiator 2,2-dimethoxyphenyl acetophenone (DMPA, Ciba Specialty Chemicals) was used in all experiments. Fig. 1 shows the chemical structures of the surfactants used in this study.

2.2. Methods

Quaternary ammonium surfactant modified clays (organoclays) were prepared as described elsewhere [17]. Briefly, appropriate amount of clay was added to deionized water and stirred vigorously. A solution containing sufficient amounts of surfactant necessary to achieve appropriately exchanged organoclay, assuming complete cation exchange, was made in a separate beaker. The surfactant solution was added to the clay mixture and stirred continuously overnight. Samples were washed several times with deionized water, centrifuged and freeze-dried. The cation exchange process was evaluated utilizing a Fourier transform infrared spectrometer (FTIR, Thermo Nicolet 679 FTIR). Absorbance peaks in the FTIR spectra characteristic of C=C double bonds (810 cm^{-1}, out of plane bending), carbonyl (1735 cm^{-1}) and methyl groups (2850 cm^{-1} and 2920 cm^{-1}) in the surfactants confirmed the presence of surfactants in the organoclay [6,8]. Thermogravimetric analysis showed greater than 85% cations exchanged based on percentage of total mass loss at 600 °C. Organoclay–monomer samples were prepared by adding appropriate amount of organoclay to the monomer in a vial and sonicating for 2 h. Formulations in which the clays were not directly exchanged were prepared by mixing clay, surfactant and monomer and sonicating for 2 h.

Photopolymerization rates were monitored using a Perkin–Elmer Diamond differential scanning calorimeter modified with a medium pressure mercury arc lamp (photo-DSC). Rates of photopolymerization were measured using the full spectrum of UV light emitted by the lamp, while neutral density filters were used to control light intensity as needed. Photopolymerization rates were calculated from the heat evolved from the reaction according to Eq. (1) [10]

$$\frac{R_p}{[M]} = \Delta Q\left[\left(\frac{M_W}{n\Delta H_p m}\right)_{\text{monomer 1}} + \left(\frac{M_W}{n\Delta H_p m}\right)_{\text{monomer 2}}\right] \quad (1)$$

where R_p is the rate of polymerization, ΔQ equals the heat evolved as measured by photo-DSC, M_W is the molecular weight of the monomer, n represents the monomer functionality, and ΔH_p is the theoretical heat of polymerization (86,200 J/mol for acrylate and 56,000 J/mol for methacrylate) [18]; m is the mass of reactive species in the formulation while [M] represents concentration of reactive species. Eq. (1) is normalized to the total reactive species concentration in the formulation to eliminate concentration effects when comparing photopolymerization rates for different formulations. Monomers 1 and 2 represent different monomers in the formulation. All polymerizations were initiated with a light intensity of 3 mW/cm^2 and 0.1 wt% photoinitiator concentration unless otherwise stated, and were conducted at room temperature.

After effect experiments to determine polymerization rate parameters were also examined following procedures described previously [19,20]. To this end, photo-DSC studies to evaluate propagation (k_p) and termination (k_t) rate parameters were conducted. Steady state polymerization rates were determined under full UV light illumination to determine k_p and k_t. All samples were irradiated with 365 nm wavelength UV light at 1 mW/cm^2. From the simplified steady state rate equation (Eq. (2)), the value of $k_p/k_t^{1/2}$ was evaluated.

$$\frac{k_p}{k_t^{1/2}} = \frac{R_p}{[M]}\frac{1}{(\phi I_o \epsilon[A])^{1/2}} \quad (2)$$

$$\frac{[M]}{R_p} = \frac{k_t}{k_p}t + \frac{[M]_o}{(R_p)_o} \quad (3)$$

R_p is the polymerization rate at time t, [M] is the molar monomer concentration, ϕ is the initiator efficiency, I_o is the initiator

extinction coefficient and [A] is the photoinitiator molar concentration in Eq. (2) [20,21].

By covering the sample at different time intervals and thereby preventing light from reaching the reacting system, the initiation step is eliminated. This allows for the evaluation of k_p/k_t according to Eq. (3), where $[M]_o/(R_p)_o$ is the polymerization rate at the instant when the light is shuttered. The slope of the plot of $[M]/R_p$ versus time yields the value of k_p/k_t. Individual propagation and termination constants were then decoupled using Eqs. (2) and (3).

Final double bond conversion was evaluated from RTIR data according to the expression: $\alpha = (A_0 - A_t)/A_0$, where α is conversion, A_0 represents absorbance at time zero and A_t is the absorbance at any time during irradiation [10]. To minimize scattering and gradient polymerization across sample depth, 15 μm samples were sandwiched between two NaCl slides and polymerized. Additionally, samples were purged for 6 min prior to initiating polymerization to reduce oxygen inhibition effects prevalent in free radical polymerizations. Small angle X-ray scattering (SAXS) studies were utilized to characterize organoclay dispersion in monomer before and after photopolymerization using a Nonius FR590 X-ray apparatus equipped with a Cu Kα radiation source at 40 kV and 30 mA [21]. Transmission electron micrographs (TEM) were collected on a JEOL JEM-1230 equipped with built-in cryogenic capability. The instrument was operated at an accelerating voltage of 120 kV. To reduce sample degradation under the electron beam, 70-nm ultramicrotomed (Leica UC6 ultramicrotome) samples were sandwiched between two 200-mesh copper grids before imaging. Samples were cryo-imaged at −120 °C.

3. Results and discussion

Lower photopolymerization rates occur in the polymerization of filled systems when large filler particles scatter, reflect or absorb the incident light required to initiate photopolymerization. This effect is shown in the photopolymerization rate profiles for increasing clay concentration in TrPGDA as a function of time (Fig. 2). The rate of photopolymerization decreases substantially upon adding 1 wt% clay to TrPGDA as compared to the unfilled formulation. Increasing clay concentration to 5 wt% results in a further 50% decrease in the rate of polymerization. Even lower rates occur with 10 wt% clay concentration. The lower photopolymerization rate on adding clay is likely due to increased light scattering and/or absorption by the large clay aggregates [22]. Such changes could also be a result of modifications to the reaction environment resulting from electron transfer to montmorillonite clay as described elsewhere [23].

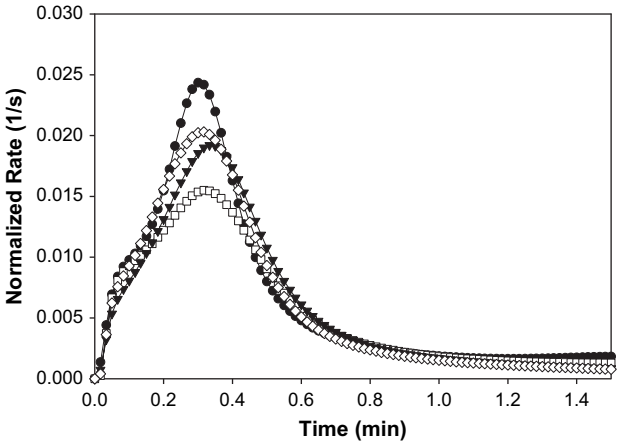

Fig. 3. Rate of photopolymerization versus time for 5 wt% clay in TrPGDA (□), with 5 wt% (▼) and 10 wt% (◇) C14MA. TrPGDA without clay or C14MA (●) is shown for comparison.

If clay agglomeration and thus interference with light penetration are reduced, it is reasonable to believe that different polymerization behavior could be observed. Additionally, the large aspect ratio of clay may influence the photopolymerization process through templating effects [12], and potential re-orientation of the reaction constituents. In polymer–clay nanocomposites, quaternary ammonium surfactants are used to modify clay surface to aid dispersion, which may potentially alter polymerization behavior, and subsequently nanocomposite properties.

To examine the polymerization behavior with added surfactants in a clay-filled formulation, both polymerizable and non-polymerizable quaternary ammonium surfactants (C14MA and TTAB, respectively) were incorporated in increasing amounts into a TrPGDA–5 wt% clay formulation. Fig. 3 shows the rate of polymerization versus time profiles for the sample containing C14MA as determined by photo-DSC. The rate of photopolymerization increases with higher C14MA concentration as compared to the clay-filled formulation. An approximately 20% increase in rate of photopolymerization over the clay-filled formulation is observed with addition of 5 wt% C14MA. Even higher C14MA concentration leads to further increases in polymerization rate. A plot of the maximum rate of photopolymerization as a function of surfactant concentration (Fig. 4) reveals that with incorporation of up to 15 wt% C14MA, the maximum polymerization rate approaches that of the neat TrPGDA formulation. This behavior is unexpected since

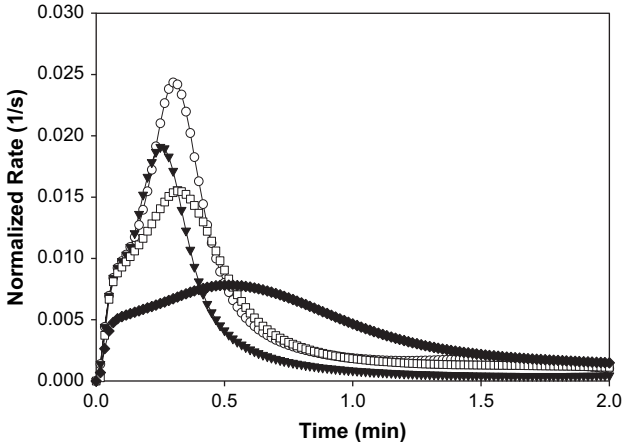

Fig. 2. Photo-DSC rate profiles of 0 wt% (○), 1 wt% (▼), 5 wt% (□) and 10 wt% clay (◆) in TrPGDA.

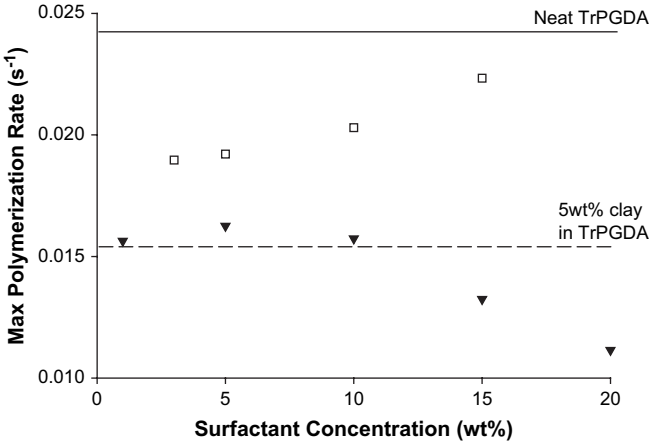

Fig. 4. Comparison of maximum rate versus surfactant concentration for addition of C14MA (□) and TTAB (▼) in 5 wt% clay–TrPGDA formulation.

copolymerizing acrylate and methacrylate species typically leads to lower rates of polymerization [21].

To understand if these increases are a result of simply adding quaternary ammonium surfactant or the presence of the reactive functionality on the quaternary ammonium surfactant, the polymerization behavior of a C14MA-containing system was compared to the non-polymerizable quaternary ammonium surfactant, TTAB (Fig. 4). The rate of photopolymerization remains relatively constant at low TTAB concentrations, but begins to decrease at higher loadings. Adding up to 10 wt% TTAB results in no significant change in photopolymerization rate in comparison to the clay-filled formulation. With TTAB concentrations higher than 10 wt%, the rate of polymerization decreases substantially. At 15 wt% TTAB concentration, a greater than 20% decrease in the maximum rate of polymerization occurs in comparison to the clay-filled system. The lower rates of photopolymerization in the TTAB samples could be due to dilution effects with increasing TTAB concentration.

The enhanced photopolymerization rate observed in the presence of polymerizable quaternary ammonium surfactant, on the other hand, suggests that the reactive functionality influences polymerization dynamics. However, the role of the nature of the surfactant can be clarified further by examining the photopolymerization behavior of monomers with similar chemical characteristics. To determine if similar increases are observed with incorporation of other methacrylates in clay, the polymerization of lauryl methacrylate (LMA), a structurally similar monomer to C14MA, was investigated in the TrPGDA–clay system.

The rate of photopolymerization as a function of time for TrPGDA–clay with increasing concentrations of LMA is shown in Fig. 5. A different polymerization behavior is observed when the quaternary ammonium surfactant is substituted with LMA. An approximately three-fold decrease in polymerization rate occurs with addition of only 5 wt% LMA to the clay–TrPGDA system. No further apparent decrease in maximum photopolymerization rate occurs when LMA concentration is further increased to 10 wt%. However, longer irradiation times are required to reach the maximum rate of photopolymerization with higher LMA concentration. This polymerization behavior suggests that the enhanced rates of polymerization could be attributed to a unique property of the polymerizable quaternary ammonium surfactant in the presence of clay particles.

The mechanism for the observed polymerization behavior for the C14MA system can be further understood by evaluating polymerization rate parameters associated with propagation and termination of free radicals during the reaction. Propagation and termination rate parameters provide insight into different mechanisms responsible for enhancing or retarding polymerization kinetics through understanding the impact on both propagation and termination processes. Analysis of polymerization behavior was conducted by examining propagation (k_p) and termination (k_t) rate parameters using aftereffect photo-DSC studies [20,21]. Differences in the rate parameters reveal changes in the polymerization mechanism that helps to elucidate the different polymerization behaviors observed in the various systems. The rate parameters were determined based on lumped acrylate–methacrylate copolymerization values.

Fig. 6a shows propagation rate parameters determined for 5 wt% C14MA or LMA in clay–TrPGDA formulation as a function of double bond conversion. The logarithm of k_p is plotted versus functional group conversion for convenience. Over the double bond conversion range studied, the propagation rate parameters exhibit similar trends and do not deviate significantly from each other in the two formulations. On the other hand, the termination rate parameters in the LMA system deviate from the C14MA system (Fig. 6b). The k_t for LMA system is higher than C14MA for double bond conversions up to approximately 25%. The rate of polymerization is highest at the lower double bond conversions. Since the propagation rate parameters are approximately the same, the higher polymerization rates can be ascribed to the lower termination rate parameters observed early in the photopolymerization of the C14MA system.

Another potential factor influencing the observed differences in the photopolymerization behavior could be related to monomer–

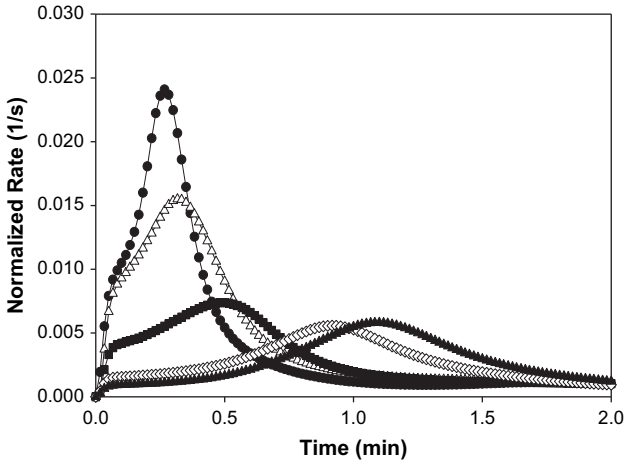

Fig. 5. Photopolymerization rate profiles of 5 wt% clay and 0 wt% (△), 1 wt% (■), 5 wt% (◇) and 10 wt% (▼) LMA in TrPGDA. TrPGDA without clay or LMA (●) is shown for comparison.

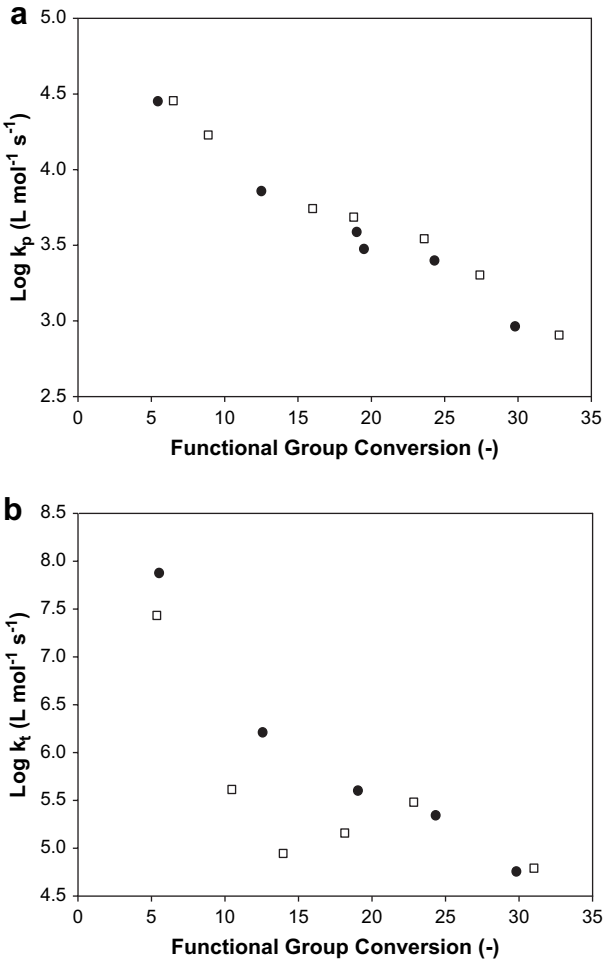

Fig. 6. (a) Propagation rate parameter ($\log k_p$) versus functional group conversion and (b) termination rate parameter ($\log k_t$) versus functional group conversion for 5 wt% clay in TrPGDA with 10 wt% LMA (●) or C14MA (□).

surfactant interactions with the clay nanoparticles that may alter the polymerization environment. The major difference between C14MA and LMA is the presence of the cation on C14MA that is capable of interacting with the clay surface. This type of association on clay surface, for instance, could result in templating effects that influence polymerization behavior as has been shown previously [12]. Changes in absorbance peaks in the 740–715 cm^{-1} region of IR spectrum have been used to monitor conformational changes in aggregates on clay surface [24]. Interactions between adjacent hydrocarbon tails from surfactants arranged in ordered, perpendicular or orthorhombic conformations result in the appearance of doublet peaks in the selected IR region. Without this type of close association between the hydrocarbon tails, singlet peaks are observed. This criterion is used to examine possible interactions between surfactants and clay nanoparticles as well as potential surfactant aggregation on the clay surfaces.

If such ordered aggregation occurs, increases in local double bond concentration may be observed that could lead to enhanced photopolymerization rates. FTIR was used to monitor changes in the absorbance peaks attributed to either C14MA or LMA in the formulation (Fig. 7). The TrPGDA–clay sample shows no distinct absorbance peak in the 740–715 cm^{-1} region of the IR spectra, indicating a lack of monomer aggregation or conformational changes within the clay–monomer system. In comparison, a single broad peak appears in the spectra of the TrPGDA–clay formulation containing 10 wt% LMA. At similar concentrations, C14MA system shows a distinct doublet peak in the specified IR region. Appearance of the doublet peak in the C14MA-filled sample indicates surfactant conformation on the clay surface. In the absence of clay, the absorbance spectra of 10 wt% C14MA in TrPGDA show a highly diffused singlet peak. This strongly suggests that the presence of clay influences the polymerization environment, and subsequently polymerization behavior. With quaternary ammonium surfactants, the clay acts as a platform for surfactant aggregation.

The lower termination rate parameters observed for C14MA formulation could be explained by considering the reaction dynamics of C14MA in the clay-filled formulation. The interaction of C14MA with the clay surface leads to immobilization of the surfactant. Due to its immobility, free radicals generated from the C14MA double bonds are limited in their ability to participate in bimolecular termination during polymerization. This behavior agrees with the observed trends in the propagation and termination rate parameters described earlier. The lower termination rates leading to higher polymerization rates observed here, also agree well with the literature on polymerization within other ordered systems [10,25–27].

Direct addition of polymerizable quaternary ammonium surfactants into clay–monomer formulations leads to faster polymerization rates that would be unexpected from copolymerizing a small amount of methacrylate in an acrylate system. While this behavior does show positive influence in photopolymerized systems, polymer–clay nanocomposites are typically prepared by using cation exchange of counterions with quaternary ammonium surfactants. As such, fundamental understanding of the photopolymerization behavior in organoclay formulations could facilitate understanding of clay morphology and structure development in a more practical environment. To study the effects of organically modified clays on photopolymerization behavior, both polymerizable and non-polymerizable organoclays were investigated. The polymerizable organoclays are either formed by cation exchange of quaternary ammonium surfactants that have a methacrylate functional group appended to the polar ammonium head (C14MA–organoclay), or attached to the end of the aliphatic tail (PM1–organoclay). TTAB modified clay was developed as a non-polymerizable analog to these organoclays. Examination of clays modified with methacrylate functional groups may allow greater understanding of surface effects in polymerization since acrylate–methacrylate copolymerization would typically lead to decreases in polymerization rates [28].

Successful cation exchange of the clay was determined using FTIR spectroscopy to characterize the absorption spectra of clay before and after organic modification. Distinct IR bands associated with –C═C–H (out of plane bending) in the methacrylate appear at 810 cm^{-1}. The –C═O peak at 1735 cm^{-1} and the symmetric and asymmetric stretch of –C–H bands at 2850 cm^{-1} and 2920 cm^{-1}, respectively, all confirm the presence of the polymerizable surfactant in the organoclay [6,23,29,30]. A similar procedure for TTAB–organoclay shows absorbance peaks indicative of –C–H moieties in the TTAB–organoclay.

To understand the photopolymerization behavior of ionically bound quaternary ammonium surfactants in acrylate formulations, polymerization rates of both polymerizable organoclays and the non-polymerizable organoclay analog that were dispersed in HDDA monomer were investigated. While unmodified clay readily disperses in TrPGDA to produce homogeneous mixtures, the organoclays used in these studies tend to form very poor mixtures in TrPGDA. Hence, the behavior of organoclays was investigated using HDDA as monomer in which the organoclays appear to be much more compatible. The photopolymerization rate profiles of different concentrations of TTAB–organoclay in HDDA are shown in Fig. 8. The rate of photopolymerization generally decreases with increasing organoclay concentration in the formulation. This

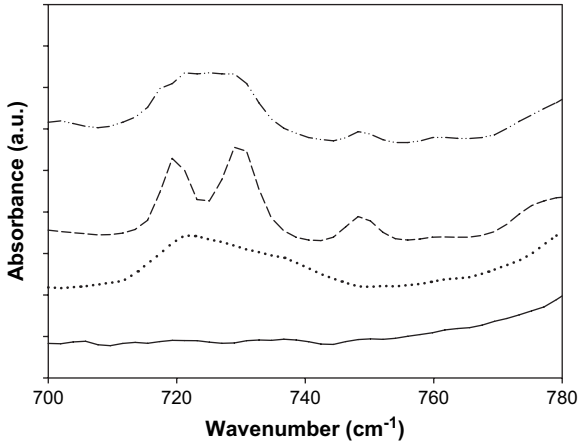

Fig. 7. Comparison of FTIR profiles of 5 wt% clay in TrPGDA (—), and 10 wt% LMA (···) or 10 wt% C14MA (– –). TrPGDA with C14MA and no clay (— · ·) is shown for comparison.

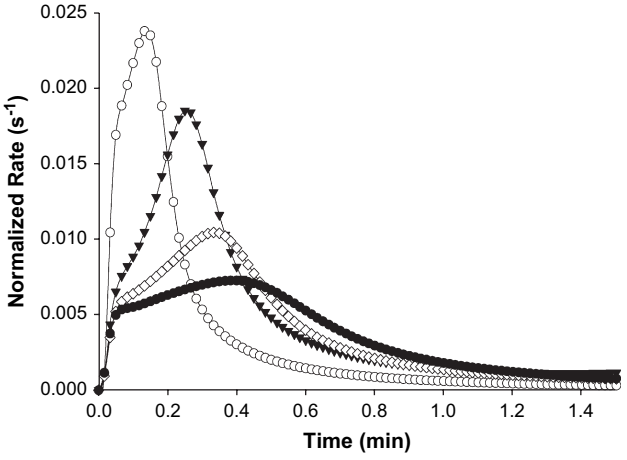

Fig. 8. Photopolymerization rate profiles of 0 wt% (○), 1 wt% (▼), 5 wt% (◇) and 10 wt% (●) TTAB–organoclay in HDDA.

behavior is similar to that observed with the addition of unmodified clay to a UV-curable system. By adding 1 wt% TTAB–organoclay to the formulation, a greater than 20% decrease in maximum photopolymerization rate is observed compared to the neat formulation. Increasing organoclay concentration results in further rate decrease, eventually reaching 60% decrease in maximum rate with 5 wt% TTAB–organoclay as compared to the neat formulation. At 10 wt% TTAB–organoclay loading, close to a four-fold decrease in the maximum rate of polymerization, as well as longer irradiation time to reach the maximum polymerization rate is observed.

To determine if the presence of a functional group on the clay surface has an influence on reaction behavior, the polymerization rate of the polymerizable organoclays in HDDA was also investigated. Fig. 9 shows the rate of photopolymerization of HDDA with added C14MA–organoclay as a function of illumination time. As observed in the TTAB–organoclay systems, adding 1 wt% C14MA–organoclay to HDDA results in lower photopolymerization rates. The extent of decrease is smaller, however, compared to the non-polymerizable surfactant system at this concentration. Further increasing C14MA–organoclay content lowers the polymerization rate even more. The maximum polymerization rate decrease for the C14MA–organoclay system is approximately 50% compared to the 60% decrease observed in the non-polymerizable system at 5 wt% organoclay concentration. Additionally, no significant difference is observed between the time to reach the maximum rate of photopolymerization, unlike the TTAB–organoclay system. A higher polymerization rate occurs at higher C14MA–organoclay concentration and suggests that higher C14MA concentration leads to increased rate in a similar fashion as adding polymerizable surfactants to the clay–monomer system.

Influence of polymerizable surfactant on photopolymerization behavior was further investigated by examining the rate profiles of PM1 exchanged clay, which has the reactive functionality attached to the end of the aliphatic chain. The reactive moiety in PM1–organoclay may allow interlayer monomer easier access to the methacrylate double bonds, leading to less overall impact on rate with organoclay addition. PM1–organoclays were photopolymerized in HDDA formulation using photo-DSC to examine polymerization rates. Fig. 10 shows the normalized rate of photopolymerization as a function of time for increasing PM1–organoclay concentrations in HDDA. The rate profiles initially exhibit similar trends as observed in the TTAB–organoclay and C14MA–organoclay systems at 1 wt% organoclay concentration. At 1 wt% PM1–organoclay concentration, the photopolymerization rate decreases compared to the neat HDDA formulation. The

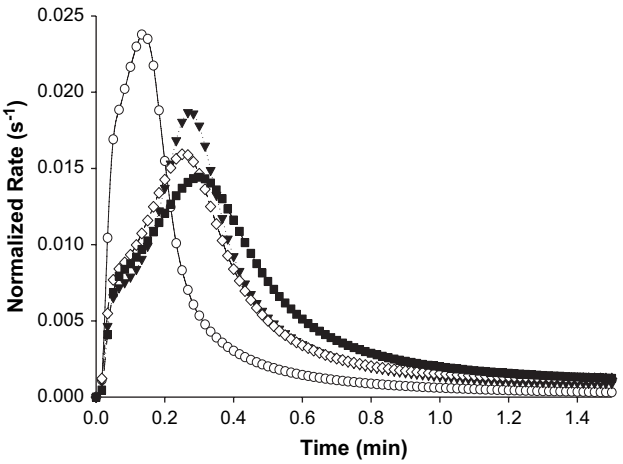

Fig. 10. Photo-DSC rate profiles of PM1–organoclay in HDDA. Shown are neat HDDA (○), 1 wt% (▼), 5 wt% (◇) and 10 wt% (■) PM1–organolcay in HDDA.

polymerization rate decreases slightly with 5 wt% PM1–organoclay concentration, with no further significant changes in the rate at even higher concentrations. However, as in the TTAB–organoclay formulation, longer times are required to reach the maximum rate of photopolymerization. The significance of the polymerizable surfactants is more evident when changes in polymerization rates with increasing organoclay concentrations are compared. While 50% and 60% decreases in rate occurs in both C14MA–organoclay and TTAB–organoclay, respectively, only a 30% decrease in polymerization rate occurs in the PM1–organoclay system at 5 wt% organoclay concentration.

The impact of polymerizable organoclays on photopolymerization behavior was investigated further by varying the amount of cations exchanged on the clay surface. A series of C14MA–organoclay formulations in which varying amounts of counterions have been exchanged with quaternary ammonium surfactants were investigated. Varying the amount of exchanged cations in organoclay increases both surfactant concentration and the organic nature of the clay nanoparticles in the polymerization medium. In addition, and perhaps more importantly, varying the amount of exchanged cations changes the amount of potentially immobilized double bonds present in the formulation. RTIR conversion profiles of 5 wt% C14MA–organoclay with 30%, 50% and 70% of the theoretical cation exchange capacity (CEC) are shown in Fig. 11. Photopolymerization reactions were carried out at low light

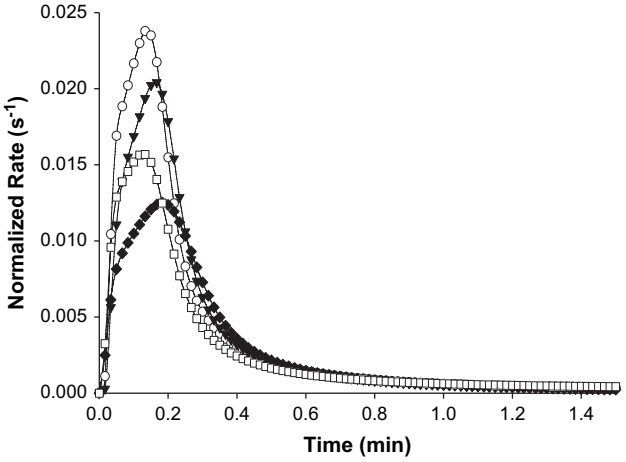

Fig. 9. Photo-DSC rate profiles of 0 wt% (○), 1 wt% (▼), 5 wt% (◆) and 10 wt% (□) C14MA–organolcay in HDDA.

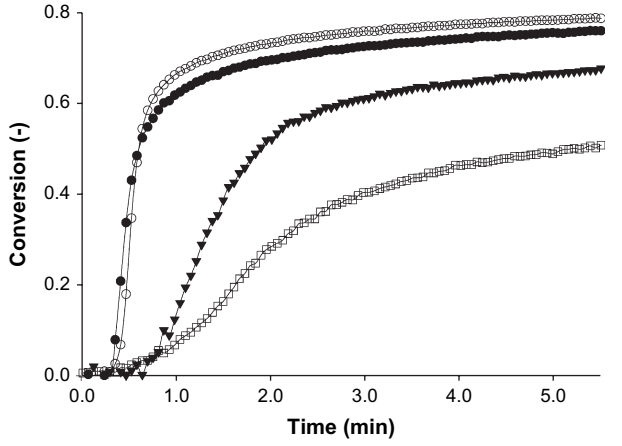

Fig. 11. RTIR plots of double bond conversion versus time for neat HDDA (○) and 5 wt% C14MA–organoclay with 30% (□), 50% (▼) and 70% (●) cations exchanged in HDDA. Polymerization was initiated with 1.0 mW/cm^2.

intensity (1.0 mW/cm^2) to highlight differences in photopolymerization behavior due to the amount of cations exchanged in the organoclay. Very low polymerization rates occur, leading to low double bond conversions (clay at 30% of the CEC). Upon exchanging more cations (50% of CEC), the final double bond conversion and rate increases. With 50% of the cations exchanged, the final double bond conversion increases to approximately 70%, but remains significantly lower than the unfilled formulation. At 70% of the cation exchange capacity, final double bond conversion increases to similar levels as the neat HDDA formulation. These changes in photopolymerization behavior could be a result of changes in the termination mechanism as discussed earlier or potentially due to changes in scattering with greater organophilic nature of the clay.

The observed differences in the photopolymerization behavior of C14MA–organoclay and PM1–organoclay systems could be related to the nature of monomer–surfactant interactions during photopolymerization. In the anchored state, accessibility to the immobilized double bonds from the surfactants is different for C14MA–organoclay and PM1–organoclays. The double bonds in PM1 are located further away from the clay surface and thus potentially more accessible to react with bulk monomer in the clay galleries. Subsequent copolymerization of PM1 species and bulk monomer could lead to decreased termination due to immobilization of the radicals. Hence, the smaller changes in polymerization rate observed in the PM1–organoclay system would be reasonable given that increasing organoclay concentration would then result in potentially higher amounts of immobilized radicals in the formulation. Polymerization rates of C14MA–organoclay systems show a greater decrease even though immobilized double bonds that copolymerize into the bulk are also available in that system. However, because the reactive functional group is located closer to the clay surface, steric effects may reduce intergallery bulk monomer–surfactant interactions. Fewer bulk monomer interactions with the immobilized C14MA double bonds and radicals may lead to the larger decreases in the observed polymerization rate compared to the PM1–organoclay system.

When the methacrylate moiety is made more accessible as in the PM1–organoclay, monomer diffusion into the clay galleries increases. Higher monomer concentrations in the clay gallery maximize the potential of reduced bimolecular termination as described earlier. Further, increased monomer diffusion into the clay galleries may result in exfoliation and lower scattering/absorption by the clay aggregates. Small angle X-ray scattering (SAXS) is a useful tool for evaluating organoclay dispersion in the monomer system. To determine differences in dispersion, SAXS studies of the different organoclay systems were performed. Fig. 12 depicts dispersion profiles of 3 wt% C14MA–organoclay and PM1–organoclay in HDDA before and after photopolymerization. The peak intensities in Fig. 12 have been offset to allow comparison in the same figure. In the PM1–organoclay profile, no primary peak is observed in the SAXS profile before and after photopolymerization. Absence of the primary peak in the PM1–organoclay profile suggests the presence of exfoliated nanoclay domains within the polymerization medium. With accessible methacrylate functional groups that are compatible with the host monomer, PM1–organoclay thus exfoliates more easily. C14MA–organoclay shows a diffused primary peak at low 2θ before photopolymerization. A decrease in intensity occurs after photopolymerization but the peak remains. Thus, C14MA–organoclay appears to retain some of the ordered clay morphology throughout polymerization, perhaps due to lack of clay interlayer compatibility with the monomer.

TEM (Fig. 13a and b) support the dispersion behavior observed in the SAXS data. Fig. 13a shows C14MA–organoclay in HDDA while Fig. 13b depicts PM1–organoclay in HDDA. Sections of the micrograph show C14MA–organoclay that appears to be exfoliated with overall C14MA–organoclay morphology showing intercalated domains with fine clay aggregates. PM1–organoclay appears better dispersed, with smaller clay aggregates that appear to be separated. It should be mentioned here that PM1–organoclay aggregates to a small degree in HDDA, but appears more highly dispersed compared to the C14MA–organoclay system.

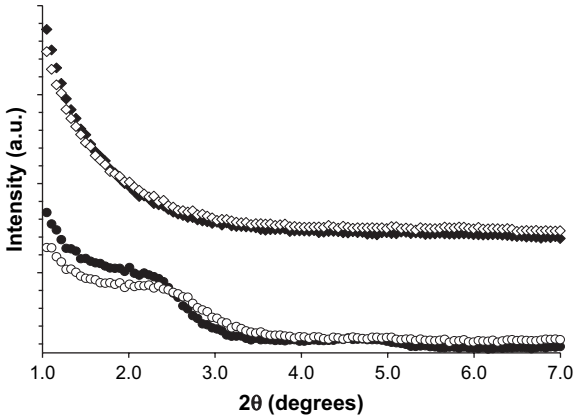

Fig. 12. SAXS profiles of 5 wt% organoclay dispersed in HDDA. Shown are unpolymerized C14MA–organoclay (●), C14MA–organoclay after polymerization (○), and PM1–organoclay before polymerization (◆) and polymerized PM1–organoclay (◇) in HDDA.

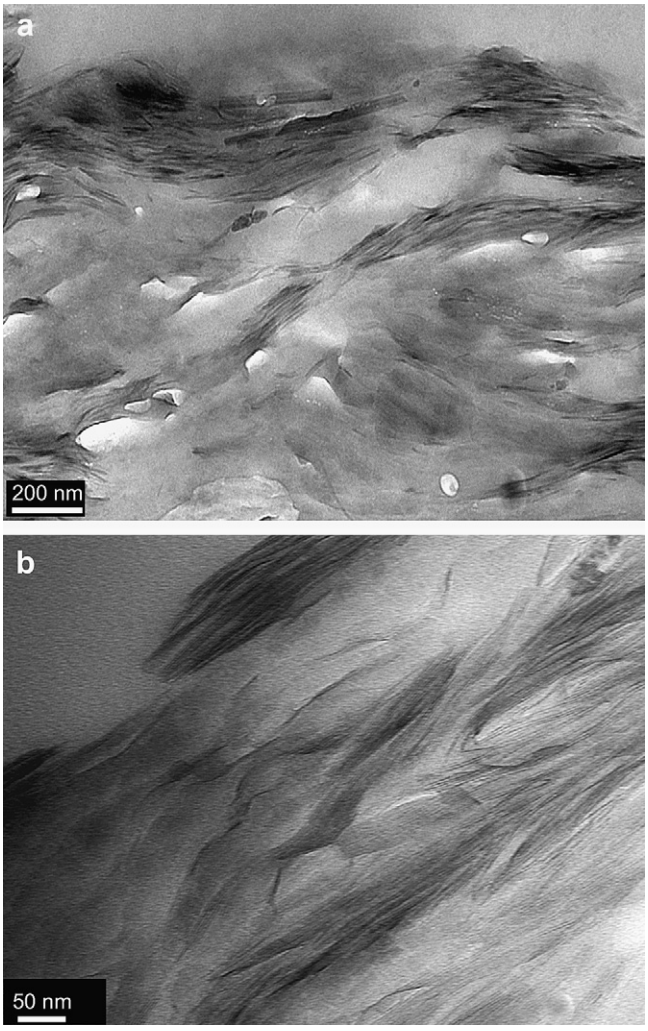

Fig. 13. TEM image of (a) 3 wt% C14MA–organoclay and (b) 3 wt% PM1–organoclay dispersed in HDDA.

Clay dispersion observed in the two polymerizable organoclay systems could affect polymerization behavior in two different ways. For PM1–organoclay, the highly exfoliated morphology could increase the ability of the bulk monomer to copolymerize with the immobilized PM1 double bonds and radicals. The result is a potential decrease in termination due to higher number of radicals on the clay surface with substantial diffusion limitations. This behavior correlates well with observations in the reaction rate parameters determined earlier. In C14MA–organoclay, intercalated clay morphology could lead to lower monomer interactions with the immobilized surfactants and limit contributions to the reaction diffusion mechanism observed in the PM1–organoclay system. Further, decreases in the size of inorganic particles because of exfoliation result in fewer interactions with the initiating light source. Subsequently, the initiation is enhanced and leads to the observed higher polymerization rates in PM1–organoclay system.

4. Conclusions

Clay morphology and interaction with various organic modifiers induce changes in polymerization behavior not realized in bulk polymerizations. Higher polymerization rates are observed as polymerizable surfactant is added to a clay–monomer system. The observed higher photopolymerization rates are due to lower termination rate parameters induced by immobilized double bonds and radicals adsorbed onto the clay surfaces, as well as ordering effects induced by the clay particles. Addition of a non-polymerizable surfactant, on the other hand, does not change polymerization rate significantly at low concentrations with large decreases at higher concentrations. Addition of non-ionic analogous methacrylate monomer also causes significantly slower polymerization rate. Organically modified clays were also modified with methacrylate functionalities for *in situ* photopolymerization. Lower photopolymerization rates are observed for increasing organoclay concentration. However, a lower overall decrease in the maximum polymerization rate occurs in formulations containing polymerizable organoclays compared to non-polymerizable systems. The nature of the polymerizable surfactant utilized affects the dispersion mechanism in the organoclays systems, which also influences photopolymerization behavior. In particular, significantly less decrease occur when the polymerizable moiety is made more accessible through exfoliation of the clay nanoparticles.

Acknowledgements

The authors acknowledge financial support from the National Science Foundation (CTS-0626395), the I/UCRC for Photopolymerization Fundamentals and Applications, and a University of Iowa AGEP fellowship.

References

[1] Giannelis EP. Adv Mater 1996;8:29.
[2] LeBaron PC, Wang Z, Pinnavaia TJ. Appl Clay Sci 1999;15:11.
[3] Alexander M, Dubois P. Mater Sci Eng 2000;28:1.
[4] Zanetti M, Lomakin S, Camino G. Macromol Mater Eng 2000;279:1.
[5] Kojima Y, Usuki A, Kawasumi M, Okada A, Fukushima Y, Karauchi T, et al. J Mater Res 1993;6:1185.
[6] Decker C, Keller L, Zahouily K, Benfarhi S. Polymer 2005;46:6640–8.
[7] Vaia RA, Giannelis EP. Macromolecules 1997;30:7990–8000.
[8] Uhl FM, Davuluri SP, Wong SC, Webster DC. Chem Mater 2004;16:1135.
[9] Clapper JD, Guymon CA. Adv Mater 2006;18:1575–80.
[10] DePierro MA, Carpenter KG, Guymon CA. Chem Mater 2006;18:5609–17.
[11] Clapper JD, Guymon CA. Macromolecules 2007;40:1101–7.
[12] Polowinski S. Prog Polym Sci 2002;27:537–77.
[13] Pindzola BA, Jin J, Gin DL. J Am Chem Soc 2003;125:2940–9.
[14] Jin J, Nguyen V, Gu W, Lu X, Elliott BJ, Gin DL. Chem Mater 2005;17:224–6.
[15] McGrath KM. Colloid Polym Sci 1996;274:499.
[16] Nagai K, Ohishi YJ. J Polym Sci Part A Polym Chem 1987;25:1–14.
[17] Park S-J, Seo D-I, Lee J-R. J Colloid Interface Sci 2002;251:160–5.
[18] Odian G. Principles of polymerization. 4th ed. Hoboken, NJ: John Wiley & Sons; 2004.
[19] Katti KS, Sikdar D, Katti DR, Ghosh P, Verma D. Polymer 2006;47:403–14.
[20] Tryson GR, Shultz AR. J Polym Sci Polym Phys Ed 1979;17:2059–75.
[21] Anseth KS, Wang CM, Bowman CN. Macromolecules 1994;27:650–5.
[22] Davidenko N, García O, Sastre R. J Appl Polym Sci 1995;97:1016–23.
[23] Solomon DH, Swift JD. J Appl Polym Sci 1967;11:2567–75.
[24] Li Y, Ishida H. Langmuir 2003;19:2479–84.
[25] Guymon CA, Bowman CN. Macromolecules 1997;30:5271–8.
[26] Lester CL, Smith SM, Jarrett WL, Guymon CA. Langmuir 2003;19:9466–72.
[27] Lester CL, Guymon CA. Polymer 2002;43:3707–15.
[28] Yousi Z, Donghai L, Lizhong D, Jinghui Z, Ronghua P. Polymer 1997;38(15): 3947–50.
[29] Tummers PHG, Houben EJE, Jansen JFGA, Wienke D. Vib Spectrosc 2007;43: 116–24.
[30] Benfarhi S, Decker C, Keller L, Zahouily K. Eur Polym J 2004;40:493–501.